Published in final edited form as:

Nat Chem Biol. ; 7(9): 595–601. doi:10.1038/nchembio.614.

Serendipitous alkylation of a Plk1 ligand uncovers a new binding channel

Fa Liu[1,5], **Jung-Eun Park**[2,5], **Wen-Jian Qian**[1], **Dan Lim**[3], **Martin Gräber**[4], **Thorsten Berg**[4], **Michael B. Yaffe**[3], **Kyung S. Lee**[2,*], and **Terrence R. Burke Jr.**[1,*]

[1] Chemical Biology Laboratory, Molecular Discovery Program, Center for Cancer Research, National Cancer Institute-Frederick, Frederick, MD 21702, U. S. A.

[2] Laboratory of Metabolism, Center for Cancer Research, National Cancer Institute, National Institutes of Health, Bethesda, MD 20892, U. S. A.

[3] Department of Biology and Biological Engineering, Center for Cancer Research, Massachusetts Institute of Technology, Cambridge, MA 02139, U. S. A.

[4] Institute of Organic Chemistry, University of Leipzig, Leipzig, Germany

Abstract

In the current work, unanticipated synthetic byproducts were obtained arising from alkylation of the δ^1 nitrogen (N3) of the histidine imidazole ring of the polo-like kinase-1 (Plk1) polo-box domain (PBD)-binding peptide PLHSpT. For the highest affinity byproduct, bearing a $C_6H_5(CH_2)_8$– group, a Plk1 PBD co-crystal structure revealed a new binding channel that had previously been occluded. An *N*-terminal PEGylated version of this peptide containing a hydrolytically-stable phosphothreonyl residue (pT) bound to the Plk1 PBD with affinity equal to the non-PEGylated parent, yet it exhibited significantly less interaction with the PBDs of the two closely-related Plk2 or Plk3. Treatment of cultured cells with this PEGylated peptide resulted in Plk1 delocalization from centrosomes and kinetochores, and chromosome misalignment that effectively induced mitotic block and apoptotic cell death. This work provides new insights that may advance efforts to develop Plk1 PBD-binding inhibitors as potential Plk1-specific anticancer therapeutic agents.

Keywords

Plk1; polo kinase; polo-box domain; crystal structure

The polo-like family of serine/threonine protein kinases (collectively, Plks) play crucial roles in cell cycle regulation and cell proliferation.[1–5] Of four human Plks (1 through 4), the

*Corresponding authors: Terrence R. Burke, Jr., Ph.D., National Cancer Institute, National Institutes of Health, Building 376 Boyles St., NCI-Frederick, Frederick, MD 21702, U. S. A. Phone: (301) 846-5906; Fax: (301) 846-6033, tburke@helix.nih.gov and Kyung S. Lee, Ph.D., National Cancer Institute, National Institutes of Health, 9000 Rockville Pike, Building 37, Room 3118, Bethesda, MD 20892, U. S. A. Phone: (301) 496-9635, Fax: (301) 496-8419, kyunglee@mail.nih.gov.

[5]These authors contributed equally to this work.

Accession codes. Protein Data Bank: Coordinates for PBD in complex with **4j** have been deposited under accession code 3RQ7.

AUTHOR CONTRIBUTIONS

F. L., J.-E. P., W.-J. Q., D. L., M. G., T. B., M. B. Y., K. S. L. and T. R. B. designed the experiments; F. L., J.-E. P., W.-J. Q., D. L. and M. G. conducted the experiments and F. L., J.-E. P., W.-J. Q., D. L., M. G., T. B., M. B. Y., K. S. L. and T. R. B. analyzed the data and wrote the paper.

COMPETING FINANCIAL INTERESTS

The authors declare no competing financial interests.

ability of Plk1 to promote oncogenic transformation[6–8] has lead to the search for inhibitors of Plk1 function that could serve as clinically relevant anticancer therapeutics.[9–16] A potential drawback of classical inhibitors directed at the Plk1 kinase domain is a lack of specificity due to the high degree of similarity in the ATP binding clefts among kinases. This could present difficulties, since down regulation of Plk1 with concomitant inhibition of the closely-related Plk2 or Plk3 would be contraindicated because of the positive roles these latter kinases play in maintaining genetic stability.[17,18]

In addition to their kinase domains, Plks also contain *C*-terminal polo-box domains (PBDs) that recognize phospho-Ser (pS)/phospho-Thr (pT)-containing motifs having *N*-proximal serine residues [S-(pT/pS)].[19–21] PBD-mediated binding provides sub-cellular localization that is critical for proper Plk function. Blockade of PBD-dependent protein-protein interactions inhibits the mitotic functions of Plk1[22–24] and the uniqueness of PBDs to Plks makes disruption of PBD-dependent interactions an alternative and potentially highly specific means of inhibiting Plk function.[6,25–27] Screening small molecule or natural product libraries represents one approach to developing Plk1 PBD-binding antagonists.[22,24,28,29] Peptide-based antagonists, derived through an understanding of PBD-ligand interactions afford a complimentary approach.

A single PBD is composed of two highly homologous polo-boxes (PB1 and PB2), each of which consists of six anti-parallel β-sheet strands and an α-helix. The association of PB1 with PB2 provides a single functional PBD composed of a 12-stranded β-sandwich that is competent to recognize and bind phoshopeptide targets.[20,21] Crystal structures of the Plk1 PBD in complex with phosphopeptides [MQSpTPL (PDB: 1Q4K),[21] PMQSpTPL (PDB: 1UMW),[20] LLCSpTPN (PDB: 3BZI),[30] LHSpTA (PDB: 3FVH),[23] PLHSpT (PDB: 3HIK),[23] and PPHSpT (PDB: 3C5L)[23]] show that the peptides bind in similar fashion within a positively-charged groove formed between the PB1 and PB2 components. Experiments indicate that a pT residue is essential for high affinity binding. Calculations showing that this residue provides approximately one third of the overall peptide binding free energy support empirical observations of its importance.[31]

In an attempt to improve the pharmacological properties of the high affinity Plk1 PBD-binding peptide PLHSpT (**1**), we previously replaced without loss of Plk1 PBD binding affinity, the hydrolytically-labile pT residue with the phosphatase-stable pT mimetic, (2*S*, 3*R*)-2-amino-3-methyl-4-phosphonobutanoic acid (Pmab)[32] (**2**).[23] More recently, we undertook the preparation of a series of pT phosphodiesters of peptide **1**, with the intent of reducing the anionic charge of the pT residue. As reported herein, during the course of these latter studies, unexpected peptide byproducts were formed that exhibited exceptional binding affinities. A co-crystal structure of the highest affinity peptide byproduct bound to Plk1 PBD unambiguously identified the structure of the byproduct as a His-adduct and revealed a new mode of binding interaction. Treatment of cultured cells with a Pmab-containing PEGylated variant of this peptide resulted in Plk1 delocalization from centrosomes and kinetochores, and chromosome misalignment that effectively induced mitotic block and apoptotic cell death. These findings could potentially be useful in the design of PBD-binding ligands.

RESULTS

Initial peptide synthesis and evaluation

In order to construct a library of phosphodiesters based on **1**,[23] we applied Mitsunobu coupling chemistries[33] to precursor peptides bound to acid-sensitive solid-phase resin. These peptides bore global protection of all reactive heteroatoms, except for a single free phosphoryl hydroxyl group, which was the intended site of condensation with substrate

alcohols (Supplementary Methods, Supplementary Results, Supplementary Fig. 1). A variety of alcohols were employed for esterification, including short alkyl chains bearing terminal diol, carboxyl, alkenyl, thiofuranyl and phenyl substituents and progressively longer *n*-alkyl-1-ols having terminal phenyl rings. The peptides were cleaved from the resin under acidic conditions and the expected phosphodiesters (**3a** – **3l**) were obtained as the main reaction products (Supplementary Fig. 1). Unexpectedly, in each case a faster eluting (HPLC) minor byproduct of unknown structure was obtained (designated as **4a** – **4l**, respectively) that exhibited a molecular weight identical to the expected product (Supplementary Fig. 1, Tables 1 and 2).

Evaluating the Plk1 PBD binding affinities of the synthetic products using an ELISA-based 96-well assay (Supplementary Methods), showed that all expected phosphodiester products **3a** – **3l** displayed measurable and in some cases, good affinity. However, the reaction byproducts (**4c** – **4l**) (with the exception of **4a** and **4b**, which were tested as mixtures with the corresponding **3a** and **3b**) uniformly displayed significantly higher affinities than their corresponding phosphodiester counterparts (Table 1; Supplementary Figs. 5 and 6). The affinities of *n*-alkylphenyl byproducts increased roughly with lengthening of the alkyl chain (with the exception of $n = 6$ and $n = 7$) and reached a maximum for $n = 8$ (**4j**). Chain extension beyond this length resulted in a reduction in binding affinity (**4k**, **4l**). Although some variation in IC_{50} values was observed from assay to assay, the affinity of the most potent analogue (**4j**) consistently exceeded that of **1** by a significant amount, that in some cases was approximately three orders-of-magnitude (**1**, IC_{50} = 36μM; **4j**, IC_{50} = 17 nM, Table 1).

Because adding long chain *n*-alkylphenyl groups to **1** introduces significant hydrophobic character, we considered the possibility that "promiscuous" mechanisms unrelated to specific interactions with the PBD could give rise to apparent high binding affinity of the byproducts.[34, 35] To address this question we made use of the fact that the "SpT" dipeptide motif is critical for specific high affinity Plk1 PBD-binding and that replacement of the serine residue by an alanine significantly reduces affinity.[20] Therefore, we prepared the corresponding analogues of **3j** and **4j** in which the serine residue was replaced with an alanine residue [**3j(S4A)** and **4j(S4A)**, respectively] and we observed that this resulted in a significant loss of affinity (Table 1). Previous work showing that high affinity peptides can retain some portion of binding affinity following serine/alanine replacement,[19] was consistent with the observed activity of the **4j(S4A)** peptide, which could be attributable to the presence of substantially increased serine-independent interactions. Overall, the data argued strongly that binding of **3j** and **4j** was specific in nature.

Identification of peptide byproducts as histidine adducts

In order to identify the structure of the highest affinity byproduct (**4j**), tandem MS analyses were performed on both **4j** and its associated phosphodiester product (**3j**) (Supplementary Methods, Supplementary Figs. 2 and 3, Tables 3 and 4). As had been anticipated, the mass spectral data for **3j** was consistent with the intended phosphodiester. However, it was found that the fragmentation of the byproduct **4j** was best explained by placement of the $C_6H_5(CH_2)_8$– group on the histidine residue. The histidine side chain consists of a (1*H*-imidazol-4-yl) ring that presents two nitrogen atoms as potential sites of alkylation. It was not possible from the tandem MS data to determine on which of the two histidine nitrogens alkylation had occurred.

Identification of a new PBD-binding channel

To unambiguously identify the site of the histidine alkylation and to understand the basis for the high binding affinity of **4j**, the co-crystal structure of Plk1 PBD in complex with **4j** was

solved (Supplementary Methods, Supplementary Table 7, Supplementary Fig. 7). This structure confirmed the earlier tandem MS results, showing that alkylation had occurred on the histidine residue. It also showed that the $C_6H_5(CH_2)_8$– group was attached to the δ^1 nitrogen (N3) on the imidazole ring. Based on this data, it is assumed that the remaining members of the **4**-series of peptides also have placement of their respective alkyl groups at this position as well.

The PBD protein backbone in the PBD•**4j** complex as well as the peptide ligand were shown to be nearly superimposable with the previously reported[23] Plk1 PBD complexed to **1** (Fig. 1a). Differences in the two structures arose primarily from the binding of the $C_6H_5(CH_2)_8$– group of **4j**, where the alkyl chain extended from the histidyl imidazole ring and traversed laterally across a series of antiparallel β-sheets (β1 – β4) of the PB1 unit. Binding interactions of the adduct occurred in a well-formed hydrophobic channel whose floor is comprised proximally by V415 (arising from the β1 sheet) and distally by F482 (arising from the αB helix) and whose opposing walls are defined by Y417 (arising from the β1 sheet) and Y485 (arising from the αB helix). The terminus of the channel is formed by L478 and Y481 (arising from the αB helix) (Supplementary Fig. 8a). Formation of this binding channel required very little movement in the side chain orientations of Y485 and F482 relative to the parent 3HIK structure and more pronounced, yet still modest movement in the side chain of Y417. However, the most dramatic movement occurred in the orientation of the Y481 aryl ring, which rotated significantly downward relative to the 3HIK structure (Fig. 1b). This movement had profound effects on the topology of the protein surface, resulting in the revelation of a new binding channel, which had previously been occluded (compare Fig. 1c and Supplementary Fig. 8b). The availability of this hydrophobic channel was unanticipated based on previous crystal structures.

Peptide PEGylation

Microinjection of the Pmab-containing peptide **2** into HeLa cells interferes with proper subcellular localization of Plk1 and induces apoptotic cell death as a result of prolonged mitotic arrest.[23, 27] However, in the current work direct incubation of **2** with cultured HeLa cells (at up to 200 μM concentration) failed to elicit a detectable cellular response. This failure was potentially due to limited intracellular bioavailability arising both from poor solubility and from low membrane transport.

Incorporation of polyethyleneglycol into a molecule (termed “PEGylation”) is known to be a valuable approach toward enhancing pharmaceutical properties.[36] Although historically, it has been applied to large constructs such as proteins (for example, see[37, 38]) and nanoparticles (for example, see[39]), the application of PEGylation to smaller entities, such as peptides (for example, see [40, 41]) and organic molecules (for example, see [42, 43]) is also known. Thus, we prepared *N*-terminal PEG conjugates of **2** (peptide **5**) and the Pmab-containing variant of **4j** (peptide **6**) as well as their serine to alanine replacement analogues for use in whole cell studies (Supplementary Methods, Supplementary Table 5, Supplementary Fig. 4). We observed that both the non-PEGylated **4j** and its PEGylated form (**6**) exhibited similar levels of PBD-binding affinities in ELISA assays (Table 1; Supplementary Fig. 6d) and in fluorescence polarization (FP) competition binding assays (Supplementary Methods, Supplementary Fig. 9, Supplementary Table 8).

Plk-binding specificity by FP techniques

To test for Plk1 specificity of the PEGylated peptides, we prepared appropriate FITC-labeled peptides (Supplementary Table 5) and performed direct FP binding assays, in which the simple construct, FITC-PEG-amide (**7**) served as a negative control (Supplementary Methods, Supplementary Fig. 10, **Table 9**). The data showed that relative to the FITC-

containing version of PEGylated-**1** (peptide **8**, K_d = 59.8 ± 4.8 nM), the Plk1 PBD-binding affinity for FITC-derivatized **6** (peptide **9**, K_d = 2.0 ± 0.2 nM) was markedly higher. (It should be noted that the K_d = 2.0 nM for peptide **9** was derived from the binding curve by using 2.0 nM of the peptide. This value is an over-estimation due to receptor depletion: The actual K_d of **9** is expected to be < 2 nM. However, precise experimental determination of this K_d would require the use of ligand concentrations < 2 nM, which are accompanied by an insufficient signal to noise ratio.) These assays also showed approximately two orders of magnitude less affinity for **9** against the Plk2 PBD (K_d = 194.2 ± 39.8 nM) and Plk3 PBD (K_d = 460.1 ± 99.2 nM) (Supplementary Table 9). Binding was PBD-specific, since deletion of the phosphoryl group in **8** [**8(pT5T)**] or introducing a serine to alanine replacement in **9** [**9(S4A)**] resulted in a significant loss of binding affinity. Specificity was also supported by results from FP competition assays using non-FITC-containing peptides, where **4j(S4A)** and **6(S4A)** showed significant affinity reductions relative to the parent peptides (Supplementary Table 8).

Cell lysate Plk pull-down assays

To compliment the FP binding results, we employed direct pull-down assays using cell lysates. For this work, we introduced an *N*-terminal Cys residue onto **1**, **1(pT5T)**, **4j** and **4j(S4A)** via linkers (peptides **10**, **10(pT5T)**, **11** and **11(S4A)**, respectively) as well as the PEGylated peptide **6** and its (S4A)-variant (peptides **12** and **12(S4A)**, respectively) (Supplementary Table 5) and then covalently conjugated the Cys residues to SulfoLink coupling resin (Supplementary Methods). Results showed that in PBD pull-down assays using transfected 293T cells, both constructs **11** and **12**, made with peptides **4j** and PEGylated **6**, interacted with Plk1 approximately 40-fold better than the parent **10**, made with control peptide **1** (Fig. 2a; Supplementary Fig. 15).

Cell culture assays

In cultured HeLa cells, we observed that **6**, but not **6(S4A)**, effectively inhibited cell proliferation in a dose-dependent manner with an IC_{50} value of 380 μM (Supplementary Fig. 11). The relatively high IC_{50} value may be due to low cell permeability, since the cellular uptake of the FITC-labeled construct (**9**) was less than 0.4% (Supplementary Fig. 12). PEGylation may have increased water solubility, thereby allowing higher concentrations of peptide to be used.

Subsequent experiments revealed that treatment of HeLa cells with 200 μM of **6**, but not **6(S4A)**, effectively induced mitotic arrest and apoptotic cell death, while treatment of cells with low concentrations (50 μM and 100 μM) of **6** induced these defects weakly (Fig. 2b, c; Supplementary Fig. 13). Compound **5**, but not **5(S4A),** also induced a weak but significant level of mitotic arrest under these conditions. As a consequence of the increasing level of apoptotic cell death following mitotic arrest, the number of arrested cells shrank at later time points (Fig. 2b–c). In contrast to the biological activities of **5** and **6**, non-PEGylated **2** and **4j** failed to exhibit a detectable level of cellular effects under the same conditions (Supplementary Fig. 13), even though their *in vitro* PBD inhibitory activities were comparable to those of their respective PEGylated forms (Table 1; Supplementary Fig. 6d). As would be expected if the observed mitotic arrest was the result of inhibition of the function of PBD, treatment of HeLa cells with **6**, but not with **6(S4A)**, induced drastic Plk1 delocalization from centrosomes and kinetochores, and severe misaligned chromosomes (Fig. 2d–e and data not shown).[44] Closely correlating with the degree of PBD binding, **5**, but not the **5(S4A)** variant, induced only mild Plk1 delocalization with a moderate level of misaligned chromosomes (Fig. 2d–e). Unlike the specific inhibition of mitotic progression by **6**, treatment of HeLa cells with a previously characterized Plk1 catalytic inhibitor, BI 2536,[13] induced a greatly delayed, but pronounced mitotic arrest and apoptotic cell death

(Fig. 2f; Supplementary Fig. 14). These observations suggest that, although more potent than **6**, BI 2536 interferes with various uncharacterized processes during the early stages of the cell cycle.

DISCUSSION

The original intent of this study was to determine whether conversion of the dianonic pT phosphoryl group to monoanionic phosphodiesters could be achieved with retention of PBD-binding affinity. Although we did find that depending on the ester group (for example **3j**, R = $C_6H_5(CH_2)_8$–), affinity equal to the parent pT-containing peptide was possible, the most significant aspect of the current work was the unanticipated finding that histidine residues bearing long chain alkylaryl groups on the δ_1 nitrogen (N3) of the imidazole ring could impart exceptional binding affinity. This affinity enhancement was achieved through new PBD-ligand interactions that took advantage of a previously occluded hydrophobic binding channel on the surface of the PBD. (While this manuscript was under review, an independent approach was reported for identifying a related binding mode.[45]) We further found that *N*-terminal PEGylation of short (5-mer) peptides did not deleteriously affect PBD-binding affinity, and that PEGylated peptides exhibited enhanced activity when given to cells in culture. The low uptake of PEGylated peptide and the observation that the potency in cellular systems is less than would be expected based solely on PBD-binding affinity, indicates that the affect of PEGylation may be to increase water solubility, rather than to increase cellular bioavailability. Although further improvement in membrane permeability is likely required to increase the efficacy of the compounds, the unexpected new binding interactions identified in this work could impact the future design of PBD-binding antagonists. Our current results provide proof-of-principle that specific inhibition of the function of Plk1 PBD is sufficient to induce mitotic arrest and apoptotic cell death. Since Plk1 over-expression is closely associated with tumorigenesis in a wide range of cancers in humans[6–8] and PBD is essentially required for Plk1 function,[46–48] this study may provide a new paradigm for the design and discovery of PBD-specific Plk1 inhibitors.

METHODS

Methods and associated references are available in the Supporting Information available on the Nature Chemical Biology website.

Supplementary Material

Refer to Web version on PubMed Central for supplementary material.

Acknowledgments

This work was supported in part by the Intramural Research Program of the NIH, Center for Cancer Research, NCI-Frederick and the National Cancer Institute, National Institutes of Health (F. L., J.-E. P., W.-J. Q., K. S. L. and T. R. B.) and National Institutes of Health grants GM60594, GM68762 and CA112967 (M. B. Y.) and the Deutsche Forschungsgemeinschaft (grant BE 4572/1-1 (T. B.). Appreciation is expressed to Marzena Dyba of the Biophysics Resource (BR) of the Structural Biophysics Laboratory, NCI-Frederick for assistance in performing MS-MS studies and to Wei Dai, New York University School of Medicine, NY for reagents. The content of this publication does not necessarily reflect the views or policies of the Department of Health and Human Services, nor does mention of trade names, commercial products, or organizations imply endorsement by the U.S. Government.

REFERENCES AND NOTES

1. Barr FA, Sillje HHW, Nigg EA. Polo-like kinases and the orchestration of cell division. Nat Rev Mol Cell Biol. 2004; 5:429–441. [PubMed: 15173822]
2. Dai W. Polo-like kinases, an introduction. Oncogene. 2005; 24:214–216. [PubMed: 15640836]

3. Lowery DM, Lim D, Yaffe MB. Structure and function of polo-like kinases. Oncogene. 2005; 24:248–259. [PubMed: 15640840]
4. van de Weerdt BCM, Medema RH. Polo-like kinases: A team in control of the division. Cell Cycle. 2006; 5:853–864. [PubMed: 16627997]
5. Archambault V, Glover DM. Polo-like kinases: conservation and divergence in their functions and regulation. Nature Rev Mol Cell Biol. 2009; 10:265–275. [PubMed: 19305416]
6. Strebhardt K, Ullrich A. Targeting polo-like kinase 1 for cancer therapy. Nature Rev Cancer. 2006; 6:321–330. [PubMed: 16557283]
7. Eckerdt F, Yuan J, Strebhardt K. Polo-like kinases and oncogenesis. Oncogene. 2005; 24:267–276. [PubMed: 15640842]
8. Takai N, Hamanaka R, Yoshimatsu J, Miyakawa I. Polo-like kinases (Plks) and cancer. Oncogene. 2005; 24:287–291. [PubMed: 15640844]
9. Goh KC, et al. PLK1 as a potential drug target in cancer therapy. Drug Dev Res. 2004; 62:349–361.
10. McInnes C, Mezna M, Fischer PM. Progress in the discovery of polo-like kinase inhibitors. Curr Top Med Chem. 2005; 5:181–197. [PubMed: 15853646]
11. Gumireddy K, et al. ON01910, a non-ATP-competitive small molecule inhibitor of Plk1, is a potent anticancer agent. Cancer Cell. 2005; 7:275–286. [PubMed: 15766665]
12. Lansing TJ, et al. In vitro biological activity of a novel small-molecule inhibitor of polo-like kinase 1. Mol Cancer Ther. 2007; 6:450–459. [PubMed: 17267659]
13. Lenart P, et al. The small-molecule inhibitor BI 2536 reveals novel insights into mitotic roles of polo-like kinase 1. Curr Biol. 2007; 17:304–315. [PubMed: 17291761]
14. Lu LY, Yu X. The balance of Polo-like kinase 1 in tumorigenesis. Cell Div. 2009; 4:4. [PubMed: 19161615]
15. Reindl W, Yuan J, Kraemer A, Strebhardt K, Berg T. A Pan-Specific Inhibitor of the Polo-Box Domains of Polo-like Kinases Arrests Cancer Cells in Mitosis. ChemBioChem. 2009; 10:1145–1148. [PubMed: 19350612]
16. Strebhardt K. Multifaceted polo-like kinases: Drug targets and antitargets for cancer therapy. Nature Rev Drug Discov. 2010; 9:643–659. [PubMed: 20671765]
17. Burns TF, Fei P, Scata KA, Dicker DT, El-Deiry WS. Silencing of the novel p53 target gene Snk/Plk2 leads to mitotic catastrophe in paclitaxel (taxol)-exposed cells. Mol Cell Biol. 2003; 23:5556–5571. [PubMed: 12897130]
18. Xie S, Xie B, Lee MY, Dai W. Regulation of cell cycle checkpoints by polo-like kinases. Oncogene. 2005; 24:277–286. [PubMed: 15640843]
19. Elia AEH, Cantley LC, Yaffe MB. Proteomic Screen Finds pSer/pThr-Binding Domain Localizing Plk1 to Mitotic Substrates. Science. 2003; 299:1228–1231. [PubMed: 12595692]
20. Elia AEH, et al. The molecular basis for phosphodependent substrate targeting and regulation of Plks by the polo-box domain. Cell. 2003; 115:83–95. [PubMed: 14532005]
21. Cheng KY, Lowe ED, Sinclair J, Nigg EA, Johnson LN. The crystal structure of the human polo-like kinase-1 polo box domain and its phospho-peptide complex. EMBO J. 2003; 22:5757–5768. [PubMed: 14592974]
22. Reindl W, Yuan J, Kraemer A, Strebhardt K, Berg T. Inhibition of Polo-like kinase 1 by blocking Polo-box domain-dependent protein-protein interactions. Chem Biol. 2008; 15:459–466. [PubMed: 18482698]
23. Yun SM, et al. Structural and functional analyses of minimal phosphopeptides targeting the polo-box domain of polo-like kinase 1. Nat Struct Mol Biol. 2009; 16:876–882. [PubMed: 19597481]
24. Watanabe N, et al. Deficiency in chromosome congression by the inhibition of Plk1 Polo box domain-dependent recognition. J Biol Chem. 2009; 284:2344–2353. [PubMed: 19033445]
25. Jang YJ, Lin CY, Ma S, Erikson RL. Functional studies on the role of the C-terminal domain of mammalian polo-like kinase. Proc Nat Acad Sci USA. 2002; 99:1984–1989. [PubMed: 11854496]
26. Lee KS, Grenfell TZ, Yarm FR, Erikson RL. Mutation of the polo-box disrupts localization and mitotic functions of the mammalian polo kinase Plk. Proc Natl Acad Sci U S A. 1998; 95:9301–9306. [PubMed: 9689075]

27. Seong YS, et al. A spindle checkpoint arrest and a cytokinesis failure by the dominant-negative polo-box domain of Plk1 in U-2 OS cells. J Biol Chem. 2002; 277:32282–32293. [PubMed: 12034729]
28. Wipf P, et al. A case study from the chemistry core of the Pittsburgh molecular library screening center: the polo-like kinase polo-box domain (Plk1-PBD). Curr Top Med Chem. 2009; 9:1194–1205. [PubMed: 19807663]
29. Li L, et al. The natural product Aristolactam AIIIa as a new ligand targeting the polo-box domain of polo-like kinase 1 potently inhibits cancer cell proliferation. Acta Pharmacol Sin. 2009; 30:1443–1453. [PubMed: 19801998]
30. Garcia-Alvarez B, de CG, Ibanez S, Bragado-Nilsson E, Montoya G. Molecular and structural basis of polo-like kinase 1 substrate recognition: implications in centrosomal localization. Proc Natl Acad Sci U S A. 2007; 104:3107–3112. [PubMed: 17307877]
31. Huggins DJ, et al. Computational analysis of phosphopeptide binding to the polo-box domain of the mitotic kinase PLK1 using molecular dynamics simulation. PLoS Comput Biol. 2010; 6:e1000880. [PubMed: 20711360]
32. Liu F, Park JE, Lee KS, Burke TR Jr. Preparation of orthogonally protected (2S,3R)-2-amino-3-methyl-4-phosphonobutyric acid (Pmab) as a phosphatase-stable phosphothreonine mimetic and its use in the synthesis of polo-box domain-binding peptides. Tetrahedron. 2009; 65:9673–9679.
33. Swamy KCK, Kumar NNB, Balaraman E, Kumar KVPP. Mitsunobu and related reactions: Advances and applications. Chem Rev. 2009; 109:2551–2651. [PubMed: 19382806]
34. McGovern SL. Promiscuous ligands. Comprehensive Medicinal Chemistry II. 2006; 2:737–752.
35. Coan KED, Maltby DA, Burlingame AL, Shoichet BK. Promiscuous aggregate-based inhibitors promote enzyme unfolding. J Med Chem. 2009; 52:2067–2075. [PubMed: 19281222]
36. Bhadra D, Bhadra S, Jain P, Jain NK. Pegnology: a review of PEG-ylated systems. Pharmazie. 2002; 57:5–29. [PubMed: 11836932]
37. Roberts MJ, Bentley MD, Harris JM. Chemistry for peptide and protein PEGylation. Adv, Drug Deliv Rev. 2002; 54:459–476. [PubMed: 12052709]
38. Pisal DS, Kosloski MP, Balu-Iyer SV. Delivery of therapeutic proteins. J Pharm Sci. 2010; 99:2557–2575. [PubMed: 20049941]
39. Tsuchida E, et al. Artificial oxygen carriers, hemoglobin vesicles and albumin-hemes, based on bioconjugate chemistry. Bioconjug Chem. 2009; 20:1419–1440. [PubMed: 19206516]
40. Miller MA, et al. Amphiphilic conjugates of human brain natriuretic peptide designed for oral delivery: In vitro activity screening. Bioconjug Chem. 2006; 17:267–274. [PubMed: 16536455]
41. Khedkar A, et al. A dose range finding study of novel oral insulin (IN-105) under fed conditions in type 2 diabetes mellitus subjects. Diabetes, Obesity and Metabolism. 2010; 12:659–664.
42. Bellouard F, Chuburu F, Yaouanc J-J, Handel H, Le Mest Y. A convenient synthetic route to polyether-tagged cyclam ligands and their nickel derivatives. Eur J Org Chem. 1999:3257–3261.
43. Kanda Y, Ashizawa T, Kawashima K, Ikeda S-i, Tamaoki T. Synthesis and antitumor activity of novel C-8 ester derivatives of leinamycin. Bioorg Med Chem Lett. 2003; 13:455–458. [PubMed: 12565949]
44. Ahonen LJ, et al. Polo-like kinase 1 creates the tension-sensing 3F3/2 phosphoepitope and modulates the association of spindle-checkpoint proteins at kinetochores. Curr Biol. 2005; 15:1078–1089. [PubMed: 15964272]
45. Śledź P, et al. From crystal packing to molecular recognition: Prediction and discovery of a binding site on the surface of polo-like kinase 1. Chem Int Ed Engl. 2011; 50:4003–4006.
46. Liu X, Erikson RL. Polo-like kinase 1 in the life and death of cancer cells. Cell Cycle. 2003; 2:424–425. [PubMed: 12963832]
47. Luo J, et al. A Genome-wide RNAi screen identifies multiple synthetic lethal interactions with the ras oncogene. Cell. 2009; 137:835–848. [PubMed: 19490893]
48. Sur S, et al. A panel of isogenic human cancer cells suggests a therapeutic approach for cancers with inactivated p53. Proc Nat Acad Sci USA. 2009; 106:3964–3969. [PubMed: 19225112]

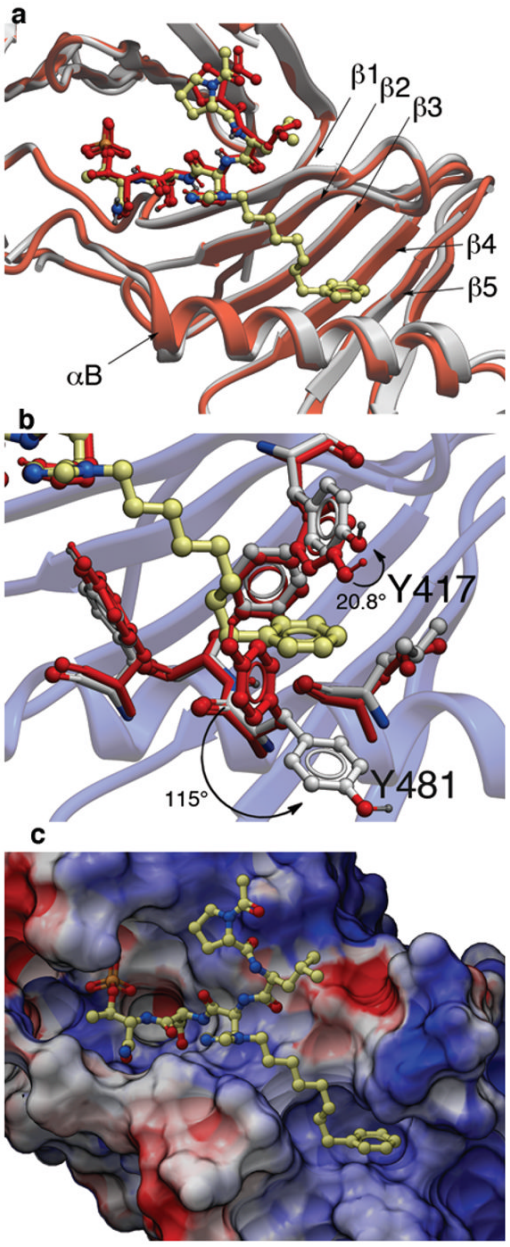

Figure 1.

X-ray co-crystal structures of Plk1 PBD complexed with peptides **1** and **4j**. (**a**) PBD in complex with **1** (PBD 3HIK; protein backbone and peptide shown in red) superimposed on the complex with **4j** (protein backbone in grey with peptide **4j** colored by atom). Key protein structural features are labeled as indicated in reference 21. (**b**) Plk1 PBD complex with **4j** (protein backbone in blue ribbon) showing residue side chains involved with the binding of the $C_6H_5(CH_2)_8$– group of **4j** (ligand in yellow with protein carbons in grey) compared with the same residues in the 3HIK structure of PBD-bound **1** (shown in red). Displacements (in degrees) are shown for the Y417 and Y481 phenyl groups. (**c**) Electrostatic surface of PBD in complex with **4j** with coloring based on an arbitrary electrostatic potential scale (positive = blue; negative = red). Peptide **4j** is rendered as thick sticks and colored by atom (blue = nitrogen; yellow = carbon; tan = phosphorus and red =

oxyben). Graphics were generated using ICM Chemist Pro by Molsoft, Inc. (www.molsoft.com).

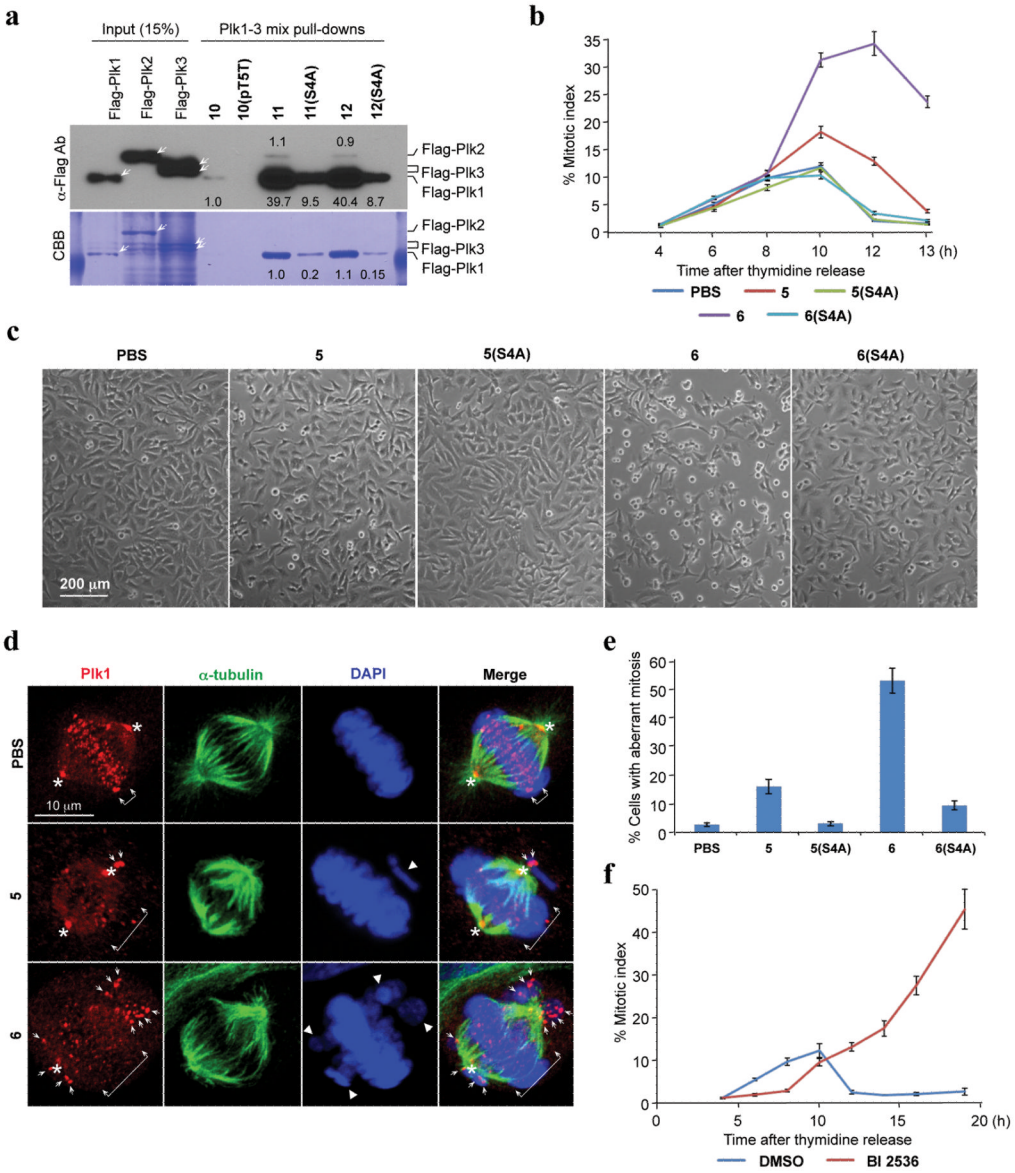

Figure 2.

Specific inhibition of the function of Plk1 PBD by peptide **6**. (**a**) Mitotic 293T cell lysates expressing kinase-inactive Flag-Plk1 (K82M), Flag-Plk2 (K108M), or Flag-Plk3 (K52R) were mixed and incubated with the indicated compounds covalently conjugated to SulfoLink coupling resin through Cys-$(CH_2)_6$-CO linker [for **10, 10(pT5T), 11**, and **11(S4A)**] or an N-terminal Cys residue [for **12** and **12(S4A)**]. Precipitates were separated, immunoblotted, and stained with Coomassie (CBB). Arrows indicate Plk1, 2, and 3 proteins. Numbers indicate the relative amounts of precipitated proteins. (**b–e**). HeLa cells released from a thymidine block and treated with 200 μM of the indicated compounds were quantified to determine the fraction of mitotic cells with rounded-up morphology (**b**). Bright-field view (**c**) and fluorescence of immunostained cells **(d)** used to quantify aberrant mitotic cells with abnormal spindle/DAPI morphologies among total mitotic population (**e**). Symbols in **(d)**: Asterisks, centrosomally-localized Plk1 signals; arrowed brackets, kineotchore-associated Plk1 signals; arrowheads, misaligned chromosomes. Note that Plk1 signals are almost completely delocalized from the centrosomes and congressed chromosomes, but rather

accumulated at the kinetochores of misaligned chromosomes near the poles, as previously described (see[48]). (**f**) HeLa cells releasing synchronously from S phase were treated with BI 2536 and analyzed (Supplementary Fig. 14). The data in **(b)**, **(e)**, and **(f)** represent mean values +/− s.d. (bars) from three independent experiments.

Table 1

Structures and Plk1 PBD binding IC_{50} values[a,b]

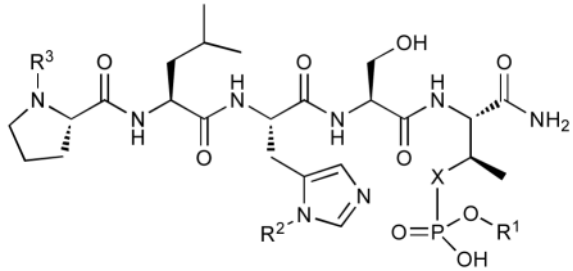

No.	X	R^1	R^2	R^3	IC_{50} (μM)
1	O	H	H	CH_3CO	36
2	CH_2	H	H	CH_3CO	174
3a	O		H	CH_3CO	>200[c]
3b	O	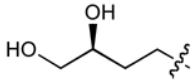	H	CH_3CO	>200[d]
3c	O	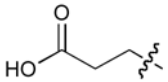	H	CH_3CO	>200
3d	O		H	CH_3CO	>200
3e	O	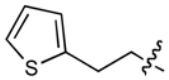	H	CH_3CO	>200
3f	O	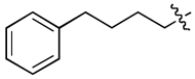	H	CH_3CO	>200
3g	O	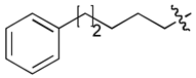	H	CH_3CO	200

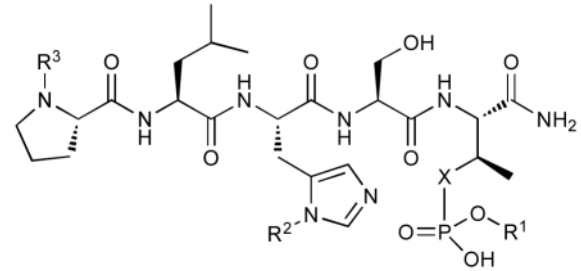

No.	X	R^1	R^2	R^3	IC_{50} (μM)
3h	O	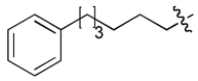	H	CH_3CO	66
3i	O	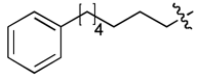	H	CH_3CO	94
3j	O	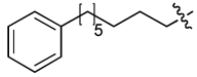	H	CH_3CO	11
3k	O	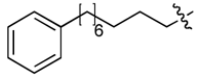	H	CH_3CO	154
3l	O	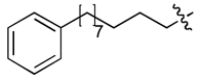	H	CH_3CO	70
4a	O	H		CH_3CO	>200[c]
4b	O	H	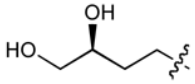	CH_3CO	>200[d]
4c	O	H	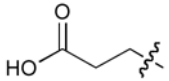	CH_3CO	>200
4d	O	H		CH_3CO	35

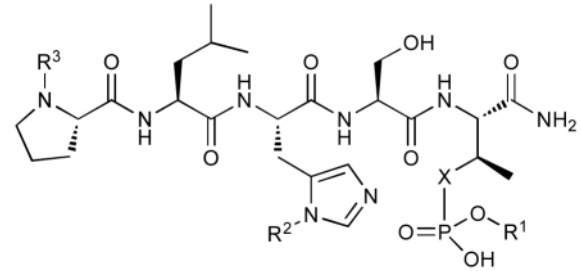

No.	X	R^1	R^2	R^3	IC_{50} (μM)
4e	O	H	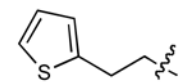	CH_3CO	19
4f	O	H	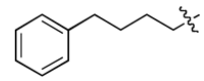	CH_3CO	11
4g	O	H	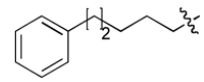	CH_3CO	4
4h	O	H	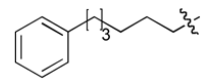	CH_3CO	0.055
4i	O	H	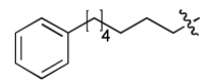	CH_3CO	0.12
4j	O	H	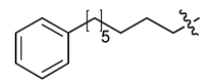	CH_3CO	0.017
4j(S4A)	O	H	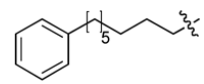	CH_3CO	12
4k	O	H	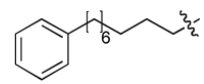	CH_3CO	0.10
4l	O	H	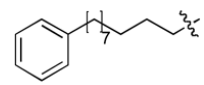	CH_3CO	0.13

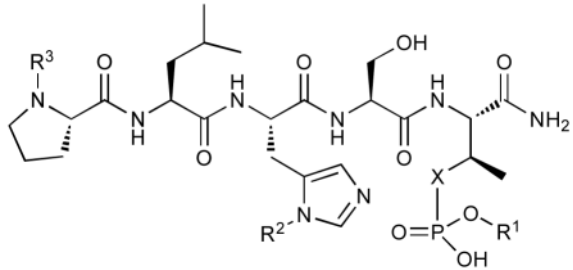

No.	X	R^1	R^2	R^3	IC_{50} (μM)
5	CH_2	H	H	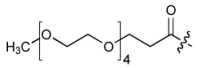	45
6	CH_2	H	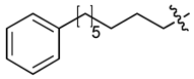	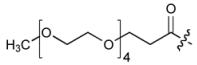	0.03
6(S4A)	CH_2	H	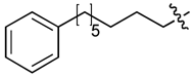	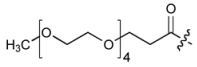	9

[a]Values were obtained from ELISA data presented in Supplementary Fig. 5 and 6. Due to assay variability, numerical IC_{50} values are for relative comparison.

[b]**1(pT5T)**, **1(S4A)**, **2(S4A)**, **3j(S4A)** and **5(S4A)** did not show detectable level inhibition at the concentrations tested.

[c]Peptides **3a**/**4a** were evaluated as a single mixture.

[d]Peptides **3b**/**4b** were evaluated as a single mixture.